Research Article

Analysis and simulation of thermal performance of a PTC with secondary reflector

Hanane Maria REGUE[1], Belkacem BOUALI[2], Toufik BENCHATTI[1], Ahmed BENCHATTI[1,*]

¹Laghouat University, Mechanical Laboratory, Laghouat, Algeria
²Laghouat University, Process Engineering Laboratory, Laghouat, Algeria

ARTICLE INFO

ABSTRACT

In this paper, a numerical simulation of fluid flow and conjugate heat transfer in a solar thermal parabolic trough collector (PTC) system is presented. The simulation is being carried out on a prototype designed in the Mechanical Laboratory in order to analyze the performance of this system. The main objective is to compare the system performance with and without a secondary reflector (SR). PVSYST software is used to provide numerical temporal values of the solar heat flux in Laghouat city (ALGERIA). Solar flux density values for four days in different seasons have been taken. SolTrace code is used to determine the heat flux distribution on the absorber tube. The conjugate heat transfer and fluid flow equations in the tube absorber are solved by using ANSYS-CFX CFD software. A comparison between two cases (traditional PTC and PTC with parabolic secondary reflector) with the same working fluid (Therminol VP-1) is carried out. The obtained results show that the system performance are practically the same for the four seasons. Moreover, the performance of the system with a second collector is better than that without a second reflector with a ratio of about 1.65.

Cite this article as: Hanane M R, Belkacem B, Toufik B, Ahmed B. Analysis and simulation of thermal performance of a PTC with secondary reflector. J Ther Eng 2021;7(6):1531–1540.

INTRODUCTION

The use of solar energy is not only related to its economic benefits, but also for its role in environments protection for which we have to find solutions to pollution problem, clean energy technology, which can help in reducing fossil-fuel consumption and carbon emissions [1]. Improved system efficiencies as well as reductions in the cost of manufacture have contributed to an increased focus on the development of CSP systems [2]. The parabolic trough concentrator (PTC) is the most popular standing for almost 90% of all CSP systems [3]. A PTC comprises an evacuated tube and a linear parabolic reflector. The evacuated tube becomes the focus of the parabolic reflector (reflective material bent into a parabolic shape). The concentrated solar beam in turn heats up the working fluid within the evacuated tube. Many academic studies have been conducted in order

---

to analyze and improve the performance of this type of energy collectors. Loni et al. [4] presented a study of thermal performance of the dish collector, which is compact system for converting solar radiation energy into thermal energy. All of the incoming solar irradiation to the dish aperture area is concentrated at the dish focal point where the solar receiver is located. The heat flux rate over each coil of the absorber is estimated by using SolTrace. This software uses the Monte Carlo ray tracing method to perform the optical analysis. Xiao et al. [5] simulated the heat flux distribution on the outer surface of the absorber tube of a parabolic solar collector receiver based on the Monte-Carlo Ray Trace (MCRT) method. The MCRT was also used by Liang et al. [6] to analyze the solar flux distribution on the receiver and the optical thermal performance of the parabolic trough collector. Islam et al. [7] investigated the optical performance of solar parabolic trough collector by considering some optical parameters. They concluded that increase in rim angle leads to an increase in non-uniform distribution of heat flux. Glass cover would increase the collection efficiency but increase the non-uniformity in flux distribution, and dislocation would lead to more uniform distribution at the lower half of receiver tube where dislocation had taken in terms of radius of receiver tube. In order to ensure that the absorber tube of the concentrator captures a maximum amount of light, a secondary reflector (SR) is essential in large aperture PTCs forming then a so-called 2-stage concentrator. Adding a SR could also, increase the concentration ratio and rim angle [8–12]. A concept of reflecting surface at an inner portion of the glass envelop has been provided by Price et al. [13]. This idea avoids the use of additional attachment for a SR, and does not require a big cost as an investment. In order to boost the concentration level, Spirkl et al. [14] proposed SRs consisting of an involute inner section followed by a flat outer section. They showed that the total concentration with these secondary concentrators reaches 77% of the theoretical upper limit for a pillbox solar distribution. Qiu et al. [15] designed and studied a linear Fresnel reflector with SR, and uses molten salt as the heat transfer fluid (HTF). Among other things, they concluded that the concentrated solar flux on the absorber surface is homogenized by the parabolic SR, which allows the utilization of all the coated surface of the absorber. Always in the same context, Wang et al. [16] presented a numerical study for a new type parabolic trough solar collector with uniform solar flux distribution. Their analysis shows that the solar flux distribution can be homogenized by adding a SR, which leads to reduce significantly the maximum temperature and the circumferential temperature difference of the absorber tube wall. An elliptical cavity geometry, as a SR, with flat plate reflector was proposed and analyzed by Cao et al. [17]. The study shows that increasing the tracking error angle and increasing the PTC focal distance would both decrease the cavity blackness. Introducing a flat plate reflector at the elliptical cavity open inlet can largely increase the cavity darkness. Recently, Sundaram and Senthil [18] conducted experiments including PTC without SR, triangular SR, and a secondary curved reflector. They have concluded that the thermal efficiency is increased by 10% and heat loss is decreased by 0.5 kW with the use of a SR. More recently, Bharti et al. [19] presented theoretical design aspects for parabolic and triangular SR and an experimental performance analysis. From the experimental analysis, the maximum temperature rise of 10.9, 9.6, and 7.4°C is observed in case of parabolic trough collector with parabolic SR, with triangular SR, and without a SR.

From the above review, we can notice the significant interest of the optical analysis and the inclusion of a SR. The present paper describes a study that has been carried out on a small-sized PTC designed in Mechanical Laboratory. The prototype is described in our previous papers [20, 21], where a series of experimental and numerical tests were made with both water and Therminol VP-1 as a working fluids. The conditions of the experiments were insufficient to generalize the study: lack of certain measuring instruments and insufficient test periods. Consequently, a preliminary simulation study, mesh independency and model validation are necessary to be able to improve the prototype in the future. The main objective of this work is the numerical simulation of conjugate heat transfer and fluid flow in the absorber tube of PTC. In order to show the interest of including SR, two cases are investigated: PTC with and without SR. PVSYST software is used to provide numerical temporal values of the solar heat flux in Laghouat region (South of Algeria). The heat flux distribution on the absorber tube is estimated by using SolTrace software, which uses Monte Carlo ray tracing method. The estimated heat flux distribution is then interpolated, by using Gaussian functions, and introduced in ANSYS-CFX solver, as a boundary condition to solve the fluid-solid conjugate heat transfer and fluid flow within the tube absorber.

DESCRIPTION OF THE STUDIED PTC

A PTC is a line-focusing system that uses a parabolic reflector to concentrate solar radiation onto a linear receiver. Reflector is one of the vital part of the PTC as it decides the fraction of solar irradiance to be collected by the absorber tube. The PTC has a length of 2 m and an area of 2×2 m². We have introduced a secondary reflector, which has a cylindrical parabolic shape, made following the same steps as the main reflector with difference in height (see Figure 1). The PTC has a single axis tracking system, from East-West and it is positioned in a South–North direction. Therminol Vp-1 is chosen as a heat transfer fluid. Table 1 summarizes the geometric characteristics of the PTC.

The concentration of energy is measured by a so-called geometrical concentration coefficient defined by the ratio

of the collector aperture A_a and the surface area of the receiver A_{abs}:

$$C = \frac{A_a}{A_{abs}} \qquad (1)$$

RAY TRACING

The distribution of heat flux over the absorber tube is vital for heat transfer analysis. Some studies have presented
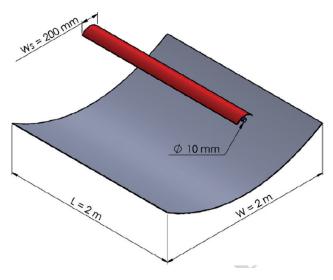

Figure 1. PTC module with secondary reflector.

that heat flux distribution over the absorber significantly affects the thermal performance of the PTC receiver [22]. In the present work, SolTrace software, which uses Monte Carlo Ray Tracing method, is used to calculate the solar flux distribution over the absorber tube.

Ray tracing simulation conditions are as follows: Sun has been modeled as a Gaussian distribution with a cone angle of 2.73 mrad. Aluminum is selected as the material of the reflector plate with a reflectivity of 1, a shape error of 3 mrad, and a specular reflection error of 0.5mrad. For the secondary reflector, the reflectivity of metal collector tube is of 0.05, the shape error is of 0.0001mrad, and the specular reflection error is of 0.0001mrad. A sample ray tracing in SolTrace is shown in Figure 2.

The solar intensity at the start of each hour (provided by PVSYST software) is introduced in Soltrace code and

Table 1. Geometrical parameters of the PTC.

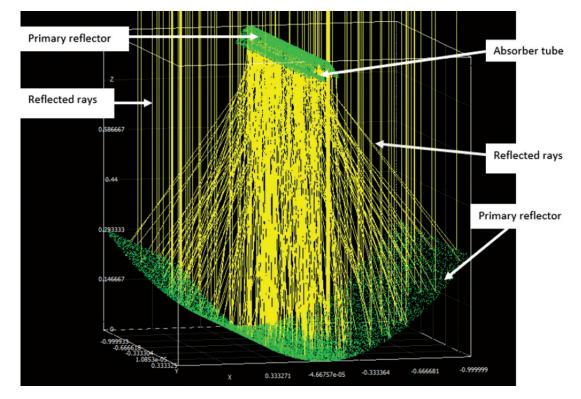|	
Focal length of the primary concentrator	0.83 m
Focal length of the secondary reflector	0.05 m
Distance between primary and secondary reflectors	0.88 m
Absorber tube inner radius	0.008 m
Absorber tube outer radius	0.01 m
Aperture width of the primary concentrator	2 m
Aperture width of the secondary concentrator	0.2 m

Figure 2. Ray tracing in SolTrace for a PTC with parabolic SR.

the outputs (data table) are interpolated by an appropriate Gaussian temporal function. Next, this function is implemented in CFX by using CEL language specific to the solver. Thereafter, it is specified as a boundary condition on the lateral surface of the tube receiver.

THERMAL MODELING

As presented by Kalogirou [2], the solar incident energy entering the parabolic trough concentrator depends on the beam solar radiation (I_b) and the aperture area of the concentrator (A_c) as given by the following relation:

$$\dot{Q}_i = A_c I_b \tag{2}$$

The optical efficiency of the system depends on the optical properties of the mirror (reflector material) such as reflectivity (R), Transmissivity (τ), absorptivity (α) of the receiver and the intercept factor (γ). It is given by the following equation:

$$\eta_0 = (R\tau\alpha) \cdot \gamma \cos\theta \tag{3}$$

Where θ is the incidence angle of the solar radiation on the aperture plane of the parabolic trough concentrator. The energy reaching the absorber surface is the combined effect of energy incident Q_i on the concentrator and optical efficiency (η_0). It is expressed as follows:

$$\dot{Q}_r = \eta_0 \cdot \dot{Q}_i \tag{4}$$

The heat loss from the absorber are composed of three terms due to conduction, convection and radiation heat losses. Therefore, the net heat exchange in the absorber is expressed as follows:

$$\dot{Q}_{net} = \dot{Q}_r - \dot{Q}_{loss,conduction} - \dot{Q}_{loss,convection} - \dot{Q}_{loss,radiation} \tag{5}$$

The efficiency is defined as the ratio of the instantaneous useful energy to the total incident radiation on the reflector aperture area.

$$\eta = \frac{\dot{Q}_{net}}{\dot{Q}_i} = \frac{\dot{m}cp(T_{out} - T_{in})}{A_C I_b(t)} \tag{6}$$

Where, $\dot{m}$ is the mass flow rate (kg/s), C_p is the specific heat capacity (J/kgK), I_b is the direct solar radiation (W/m²), Tout is the outlet temperature of the HTF, Tin is the inlet temperature of the HTF, and A_c is the aperture area of the collector. A_c is given as follows

$$A_c = W \cdot L \tag{7}$$

Where W is the width aperture of the collector, L is the length of the collector, and A_c is the aperture area of the collector.

Governing Equations

Fluid flow and heat transfer in both domains solid and fluid are described by a system of four equations to be simultaneously solved. This system is presented hereafter [23]:

- **Continuity**

$$\frac{\partial \rho}{\partial t} + \nabla(\rho U) = 0 \tag{8}$$

- **Momentum**

$$\frac{\partial(\rho U)}{\partial t} + \nabla \cdot (\rho U \otimes U) = -\nabla p + \mu \nabla \cdot \nabla U \tag{9}$$

- **Thermal energy**

$$\frac{\partial(\rho h)}{\partial t} + \nabla(\rho U h) = \nabla \cdot (\lambda \nabla T) \tag{10}$$

Where, U is the velocity vector, p is the fluid pressure, T is the temperature and h is the enthalpy.

Note that equation (10) is applied for both domains fluid and solid (for conduction in the solid, the left term in equation 10 is zero).

Materials Properties

In this work, the materials in question are copper for the tube and Therminol VP-1 for the working fluid. Copper physical properties are predefined in CFX solver. Therminol VP-1 properties (Density, Thermal Conductivity, Heat Capacity and Viscosity) are tabulated in Ref. [24] according to the temperature. In order to implement fluid properties in the solver we use interpolation functions. Accordingly, these properties are described by the following equations:

$$\rho(kg/m^3) = -6.44 \times 10^{-9}T^4 + 3.268 \times 10^{-6}T^3 \\ - 8.191 \times 10^{-4}T^2 - 0.7469T + 1079 \tag{11}$$

$$\lambda\,(W/m \cdot K) = -1.78 \times 10^{-7}T^2 - 8.432 \times 10^{-5}T \\ + 0.1378 \tag{12}$$

$$Cp(J/kg \cdot K) = 1593 \exp(0.001254T) \\ - 120.8 \exp(-0.01471T) \tag{13}$$

$$\mu(Pa \cdot s) = 5.805 \times 10^{-3} \exp(-0.03133T) \\ + 1.402 \times 10^{-3} \exp(-0.006729T) \tag{14}$$

Where T is in the range [12–425]°C.

The previous properties equations are implemented in the solver as expressions by using CFX Expression Language (CEL) specific to CFX software.

MESH INDEPENDENCY

The mesh size is selected in order to minimize the CPU time and to achieve the desired accuracy. In other words, we must find the limit from which the solution is independent of the mesh refinement for a given accuracy of calculation. In the present work, we have followed the recommendations presented by Tu et al. [25]. First, acceptable precision must be predefined (10^{-4} in terms of RMSE) for all variables. Then a series of five meshes are generated (see Table 1). The solution to be compared (target solution) is the fluid outlet temperature. As it can be seen in Figure 3, starting from mesh 3 the solution becomes independent from the mesh refinement. Table 2 illustrates the meshes characteristics.

INITIAL AND BOUNDARY CONDITIONS

Before solving the governing equations, domain initialization and boundary conditions must be specified. The domain is initialized as follows: At time t = 0s, we consider that the fluid and the solid are at the same temperature T_0; the fluid velocity is set to zero, and the pressure is set to 38 kPa (which is greater than the saturation pressure at the maximum obtained temperature, 275°C). The boundary

Table 2. Characteristics of meshes used for the mesh independency study

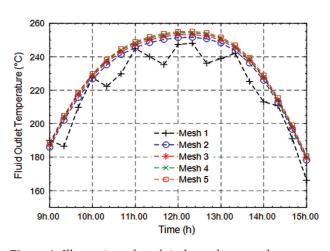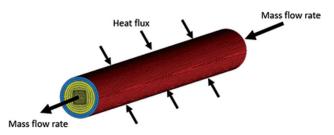| Mesh	Refinement ratio	Element number	Calculation time
M1	1.5	22000	1min 32s
M2	1.5	60000	3min 5s
M3	1.5	144000	6min 6s
M4	1.5	264000	10min10s
M5	1.5	416000	17min 34s

Figure 3. Illustration of mesh independence study.

conditions are illustrated in Figure 4. The mass flow rate across the tube is chosen to ensure a laminar flow within the tube. In addition, the pressure at the outlet of the tube should not reach the fluid saturation pressure. This is determined based on the relation between mass flow rate and pressure drop for a laminar flow in a cylindrical tube.

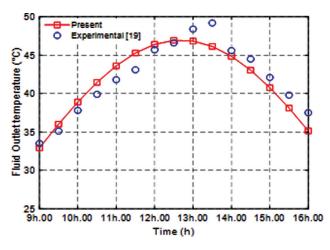## RESULTS AND DISCUSSION

Model Validation

To be able to analyze the performance of a PTC using the proposed model, it is important to validate it. For this purpose, the model is applied to the system described in reference [19]. It is a small-sized PTC equipped with two types of second reflector, the triangular reflector and the parabolic reflector. Here we are only interested by the parabolic reflector. The simulation results are compared with experimental results reported in this reference. The results to be compared are the fluid (water) temperature at the absorber tube outlet.

Figure 4. Illustration of the boundary conditions applied on the absorber.

Table 3. Experimental data for PTC with parabolic secondary reflector [19]

Time (h)	$I_b (W/m^2)$	T_{in} (°C)	T_{out} (°C)
09.00	399.1	29.5	33.5
09.30	489.2	29.6	35.1
10.00	598.7	29.6	37.8
10.30	687.4	29.8	39.9
11.00	688.3	30.1	41.8
11.30	737.4	30.2	43.1
12.00	859.8	30.9	45.7
12.30	862.6	31.5	46.6
13.00	826.0	31.8	48.4
13.30	746.2	31.9	49.2
14.00	653.5	31.6	45.6
14.30	547.3	33.3	44.5
15.00	447.4	33.4	42.1
15.30	330.1	33.0	39.8
16.00	227.0	33.2	37.5

Figure 5. Fluid outlet temperature versus time. Comparison between experimental data and simulation results.

Figure 6. Variation of modeled solar radiation with time for 4 months in region of Laghouat.

The absorber tube has the following dimensions: inner diameter 10.7 mm, outer diameter 12.7 mm, and length 2.5 m. The data and tests results are summarized in Table 3. Note that, these tests have been performed on 03/05/2018. The obtained results for the fluid outlet temperature are presented in Figure 5. As it can be seen, the maximum temperature value obtained by simulation is slightly deviated to the left compared to the experimental value. This is due to the calculation errors, the conditions of the experiment, as well as to the energy storage. However, Error range recorded is about 2.73°C (maximum deviation), the mean absolute error is about 1.43°C, the standard deviation is 0.74, and the root mean square error is 1.56. According to these values, we can conclude that the present model is in good agreement with the experimental data. Therefore, the model can be used to analyze the optical and thermal performance of PTC.
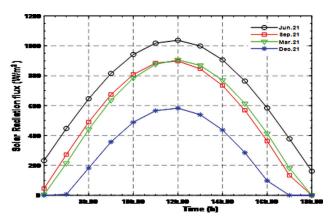
Solar Radiation

Figure 6 represents the solar radiation as a function of time for 4 days from four months (March 21, June 21, September 21 and December 21). The numerical temporal intensity of solar radiation are obtained by using PVSYST5 software for a location (2°56 Longitude and 33°46 Latitude).

Optical Modeling

The main objective of the optical modeling is to determine the concentration of power in the absorber tube, and the evolution of the heat flux at the absorber according to a variation of the incidence angle of solar rays.

Figures 7(a) and (b) show consecutively the contour and the surface plot of the average heat flux intensity. The average heat flux density of receiver is 80000 W/m², which is numerically simulated using SolTrace software. Simulation model and heat density distribution with the direct normal irradiance of 1000 W/m² are shown in Figure 7 (a).

Figure 7 (b) represents plot paths of ray in the range 1–100 rays. The result of average heat flux density of the collector is 88249W/m².
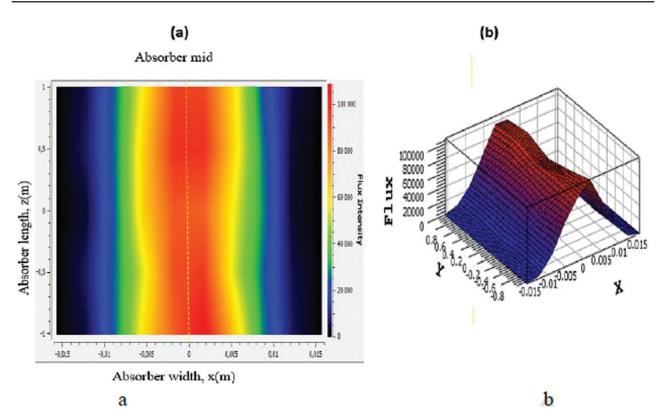
Figure 8 shows the heat flux distribution on the circumference of absorber tube obtained by ray tracing. The value of heat flux for the case (b) is high on around all the absorber tube due to concentrated of the primary reflector and secondary one. The maximum radiation obtained is about 80000 W/m². A non-linear heat flux distribution is observed over the absorber, which leads to a high temperature gradient. The value of heat flux for the case (b) is high on the lower portion of the absorber tube due to concentrated solar flux so and low on the upper portion due to direct sunlight for the absorber.

Fluid Temperature

The variations of the temperature, at the tube outlet, during different days are represented in Figure 9 for both cases: with and without secondary reflector. As it can be seen, the fluid temperature at the outlet of the absorber tube is proportional to the direct sunlight. As the density of the solar flux increases, the temperature of the fluid increases until it reaches the maximum. Then, it decreases with the solar flux until the end of the day. It mainly depends on the heat quantity absorbed by the tube, which is based on optical and geometric parameters of concentrator. We note that for every day and in both cases, the temperature pick is reached around 12.00 h. We also notice a difference in maximum temperatures (June) of about 90°C and in minimum temperatures (December) about 50°C between the two cases.

Useful Thermal Energy

The Therminol VP-1 oil is used as heat carrier fluid. During the simulation, the physical properties of the heat carrier fluid are varied depending on the temperature of the

Figure 7. Plot of heat flux for a parabolic trough collector with SR, (a) contour plot on the tube absorber upper surface, (b) surface plot.
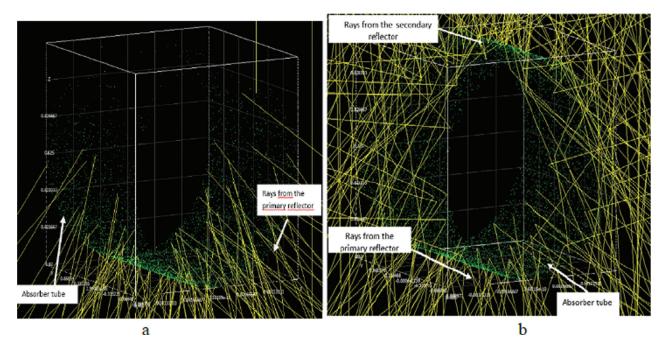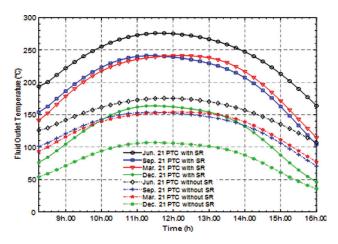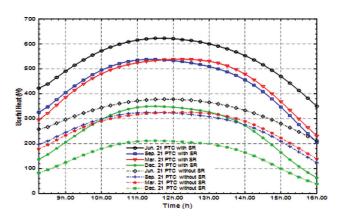

Figure 8. Rays incident on the absorber for (a) without SR (b) with SR.

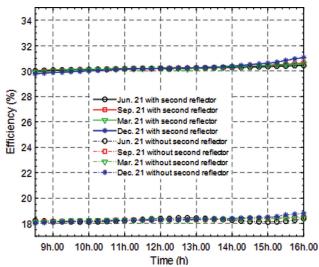**Figure 9.** Variation of fluid temperature at the tube outlet versus time.

Figure 10. Variation of useful thermal energy with respect to time.

Figure 11. Variation of instantaneous thermal efficiency versus time.

Table 4. Performance comparison between PTCs with and without secondary reflector

	Mean Efficiency (%)		
	PTC with second reflector	**PTC without second reflector**	**Ratio**
June 21	30.2	18.3	1.65
September 21	30.2	18.3	1.65
December 21	30.2	18.3	1.65
March 21	30.2	18.3	1.65

fluid according to equations (11) to (14). Variations of the heat transported by the carrier fluid are shown in Figure 10. We notice that the variation profiles are similar to those of the temperature at the tube outlet. We also note that the difference in useful heat between the two cases (a) and (b) is about 540 W during the month of June and 140 W during the month of December.

Thermal efficiency

The PTC thermal efficiency values obtained by numerical simulation are reported in Figure 11. As it can be seen, the efficiency is approximately constant equal to 30 % for a PTC with secondary reflector in all seasons. For a PTC without secondary reflector, the efficiency is around 18% in the four seasons. We record then a ratio of 1.65 between the two cases as shown in Table 4.

In order to increase the PTC efficiency, further studies can be investigated focusing especially on the solar energy storage by application of phase change materials such as described in reference [26].

CONCLUSION

In this paper, an analysis and simulation of thermal performance of a small sized PTC is performed. Two cases are the subject of the simulation: PTC with and without secondary reflector. The simulation is conducted on four different days of the four seasons. Monte Carlo Ray Tracing method is used to calculate the solar flux distribution over the absorber tube. Conjugate heat transfer and fluid flow within the tube are solved by using ANSYS-CFX solver. Oil Therminol VP-1 is used as a carrier fluid and its physical properties according to temperature are implemented in the solver. The obtained results showed the followings:

- The PTC efficiency is constant for the four seasons in both studied cases.
- The advantage of using a secondary reflector is that the heat flux around the receiver tube is distributed more uniformly.
- The performance of the system with a second reflector is better than that without a second reflector with a ratio of about 1.65.

NOMENCLATURE

A_c aperture area of the concentrator, m^2
C_p specific heat of heat transfer fluid, J/kg.K
D asorber tube diameter, m
I_b solar irradiance, W/m^2
L length of absorber tube, m
p presure, Pa
Q_{loss} loss rate of heat loss from the cavity receiver, W
R reflectivity
T temperature, K
T_{in} inlet temperature of heat transfer fluid, K
T_{out} outlet temperature of heat transfer fluid, K
U velicoty, m/s
W primary reflector width, m
$\dot{Q}_t$ solar incident energy entering the parabolic trough concentrator, W
$\dot{Q}_{net}$ net heat transfer rate, W
$\dot{Q}_r$ heat gained by heat transfer fluid, W
$\dot{Q}_u$ useful heat gain by the HTF in the receiver, W
$\dot{m}$ mass flow rate of heat transfer fluid, kg/s

Greeks Letters
α absorptivity of the receiver
η instantaneous thermal efficiency
η_o optical efficiency
θ incidence angle of the solar radiation
μ dynamic viscosity, kg/m.s
ρ density, kg/m^3
τ transmitivity of the receiver
λ thermal condictivity W/m.K

AUTHORSHIP CONTRIBUTIONS

Authors equally contributed to this work.

DATA AVAILABILITY STATEMENT

No new data were created in this study. The published publication includes all graphics collected or developed during the study.

CONFLICT OF INTEREST

The author declared no potential conflicts of interest with respect to the research, authorship, and/or publication of this article.

ETHICS

There are no ethical issues with the publication of this manuscript.

REFERENCES

[1] Wang YP, Shi XS, Huang QW, Cui Y, Kang X. Experimental study on direct-contact liquid film cooling simulated dense-array solar cells in high concentrating photovoltaic system. Energy Conversion and Management 2017;135:55–62. [CrossrRef]

[2] Kalogirou SA. Solar thermal collectors and applications. Progress in Energy and Combustion Science 2004;30:231–295. [CrossrRef]

[3] Frank L. Overview of parabolic troughs and linear Fresnel receivers. IEA CSP workshop March 2014:1–16.

[4] Loni R, Kasaeian AB, Askari Asli-Ardeh E, Ghobadian B, Najafi G. Comparion study of air and thermal oil application in a solar cavity receiver. Journal of Thermal Engineering 2019;5:221–229. [CrossrRef]

[5] Xiao J, He Y, Cheng Z, Tao Y, Xu R. Performance analysis of parabolic trough solar collector. Journal of Engineering Thermophysics 2009;30:729–733

[6] Liang H, You S, Zhang H. Comparison of three optical models and analysis of geometric parameters for parabolic trough solar collectors. Energy 2016;96:37–47. [CrossrRef]

[7] Islam M, Miller S, Yarlagadda P, Karim A. Investigation of the effect of physical and optical trough collector. Energies 2017;10:1907. [CrossrRef]

[8] Collares-Pereira M, Gordon JM, Rabl A, Winston R. High concentration two-stage optical for parabolic trough solar collectors with tubular absorber and large rim angle. Solar Energy 1991;47:457–466. [CrossrRef]

[9] Bennett W, Lun J, Jonathan F, Roland W. Experimental performance of a two-stage (50X) parabolic trough collector tested to 650°C using a suspended particulate (alumina) HTF. Applied Energy 2018;222:228–243. [CrossrRef]

[10] Bennett W, Lun J, Jonathan F. Theoretical and experimental performance of a two-stage (50X) hybrid spectrum splitting solar collector tested to 600°C. Applied Energy 2019;239:514–525. [CrossrRef]

[11] Mahmoud A, Bennett KW, Lun J. Novel double-stage high-concentrated solar hybrid photovoltaic/ thermal (PV/T) collector with nonimaging optics and GaAs solar cells reflector. Applied Energy 2016;182:68–79. [CrossrRef]

[12] Evangelos B, Christos T. Alternative designs of parabolic trough solar collectors. Progress in Energy and Combustion Science 2019;71:81–117. [CrossrRef]

[13] Price H, Lüpfert E, Kearney D, Zarza E, Cohen G, Gee R, et al. Advances in parabolic trough solar power technology. Journal of Solar Energy Engineering 2002;124:109. [CrossrRef]

[14] Spirkl W, Ries H, Muschaweck J, Timinger A. Optimized compact secondary reflectors for

parabolic troughs with tubular absorbers. Solar Energy 1997;61:153–158. [CrossrRef]

[15]   Qiu Y, Ze YL, Cheng ZD, Wang K. Study on optical and thermal performance of a linear Fresnel solar reflector using molten salt as HTF with MCRT and FVM methods. Applied Energy 2015;146:162–173. [CrossrRef]

[16]   Wang, K, He Y, Cheng Z. A design method and numerical study for a new type parabolic trough solar collector with uniform solar flux distribution. Science China Technological Sciences 2014;57:531–540. [CrossrRef]

[17]   Cao F, Wang L, Zhu T. Design and optimization of elliptical cavity tube receivers in the parabolic trough solar collector. International Journal of Photoenergy 2017;1471594. [CrossrRef]

[18]   Sundaram P, Senthil R. Thermal performance enhancement of solar parabolic trough collector using secondary reflector. International Journal of Engineering and Technology 2017;8:2964–2969. [CrossrRef]

[19]   Bharti A, Mishra A, Bireswar P. Thermal performance analysis of small-sized solar parabolic trough collector using secondary reflectors. International Journal of Sustainable Energy 2019:38:1002–1022 [CrossrRef]

[20]   Regue HM, Benchatti T, Medjelled H. Improving the performances of a solar cylindrical parabolic dual reflection mirror experimental part. International Journal of Heat and Technology 2014;32:171–178

[21]   Regue HM, Bouali B, Benchatti T, Benchatti A. Numerical simulation of conjugate heat transfer in a ptc with secondary reflector. International Journal of Heat and Technology 2020;38:9–16

[22]   Wendelin T. SolTRACE: A new optical modeling tool for concentrating solar optics. Proceedings of ISEC 2003;4490:253–260. [CrossrRef]

[23]   ANSYS-CFX Theory Guide. (2019). Southpointe: ANSYS Inc. Avaialable at: http://www.pmt.usp.br/academic/martoran/notasmodelosgrad/ANSYS%20Fluent%20Theory%20Guide%2015.pdf

[24]   Therminol VP-1. Vapor Phase/ Liquid Phase Heat Transfer Fluid (Liquid Phase), Solutia Inc, 2017. Available at: http://twt.mpei.ac.ru/tthb/hedh/htf-vp1.pdf/, Accessed on Mar 12, 2018.

[25]   Tu J, Yeoh GH, Liu C. Computational Fluid Dynamics, a Practical Approach. 2nd ed. Amsterdam, Netherlands: Butterworth-Heinemann, Elsevier, 2013.

[26]   Gurupatham SK, Manikandan GK, Fahad F. Harnessing and storing solar thermal energy using phase change material (pcm) in a small flat plate collector. Journal of Thermal Engineering 2020;6:511–520.